# Joint Adaptive M-QAM Modulation and Power Adaptation for a Downlink NOMA Network

Wenjuan Yu, *Member, IEEE*, Haowei Jia, Leila Musavian, *Member, IEEE*

***Abstract*—In this paper, we study joint adaptive M-QAM modulation and power adaptation for a downlink two-user non-orthogonal multiple access (NOMA) network. Without sacrificing bit error rate (BER), joint adaptive transmission can fully utilize the time-varying nature of wireless channels, by allowing both power and rate to adapt to channel fading. Two adaptive power allocation strategies, namely, *Scheme 1* and *Scheme 2*, each of which guarantees the minimum target rate for one user while supporting the highest possible rate for the other, are first proposed. Then, based on the two power schemes, the performance of joint adaptive transmission in terms of average spectral efficiency (SE) is studied for continuous-rate and discrete-rate modulation, while guaranteeing the minimum required rate and BER requirements. With the focus on practical discrete-rate M-QAM modulation, it is proved that for the strong user in *Scheme 1* and the weak user in *Scheme 2*, their average SEs converge to the minimum target rates. In order to further increase the total transmission rate, we then propose a dynamic rate and power adaptation (DRPA) algorithm, aiming to increase the rate of one user without sacrificing the rate of the other. It is shown that at high SNRs, the DRPA algorithm allows the strong user in *Scheme 1* and the weak user in *Scheme 2* to continue to increase their transmission rates until reaching the highest modulation order that the system can support. Hence, the total transmission rate can be greatly increased at high SNRs due to the adoption of DRPA, by allowing both users in each scheme to reach the highest transmission rate in the system.**

***Index Terms*—Adaptive modulation, power adaptation, M-QAM, NOMA, spectral efficiency.**

## I. Introduction

Due to its high spectral efficiency (SE) performance by simultaneously serving multiple users within the same radio resource, power-domain non-orthogonal multiple access (NOMA) has been viewed as a promising multiple access technique for future communication networks [1]. For power-domain NOMA[1], superposition coding is the key technology at the transmitter to perform user-multiplexing, while multiuser separation techniques such as successive interference cancellation (SIC) are required at the receiver to decode the message [2]. In the literature, there are many research efforts devoted to improving SE and energy efficiency [3]–[5], studying security performance [6]–[8], analyzing delay-constrained rate [2], [9], investigating user scheduling [10], and enhancing computation efficiency in NOMA-aided mobile edge computing [11]. Furthermore, driven by the heterogeneous service requirements in beyond 5G era, NOMA can be beneficial by enabling flexible scheduling and leveraging diversified Quality of Service (QoS) requirements across services to ensure performance guarantees [12]. Another popular research direction in NOMA in recent years is the NOMA-enabled random access (NOMA-RA). With the ability to accommodate multiple transmissions on one resource block, NOMA appears to be an attractive solution to support massive machine type communication (mMTC). Many research articles study how to incorporate code-domain NOMA or power-domain NOMA into contention-based random access techniques such as pure ALOHA and slotted ALOHA [13]–[17]. It has been found that when there are four power levels, the maximum throughput of NOMA-RA achieves over three times that of the conventional slotted-ALOHA [17], which is seen as a substantial improvement.

However, most research studies on NOMA are based on Shannon theory, without placing any restriction on the complexity or delay of the multiplexed transmission scheme [18]. Shannon capacity only serves as a theoretical upper bound on the data rates that can be achieved. Instead of studying Shannon limit, in this paper, we focus on the average SE with bit error rate (BER) guarantees and practical modulation methods for a downlink NOMA network. Furthermore, in most of the

This work has been funded by the European Union Horizon 2020, RISE 2018 scheme (H2020-MSCA-RISE-2018) under the Marie Sklodowska-Curie grant agreement No. 823903 (RECENT).

W. Yu is with the School of Computing and Communications, InfoLab21, Lancaster University, LA1 4WA, U.K. (Email: w.yu8@lancaster.ac.uk) H. Jia is with Sichuan Highway Transportation & Communication Project Co., Ltd., China. (Email: haowei_jia@outlook.com) L. Musavian is with the School of Computer Science and Electronic Engineering, University of Essex, CO4 3SQ, U.K. (Email: leila.musavian@essex.ac.uk)

[1]The power-domain NOMA is hereafter referred to as NOMA for simplicity.

performance analysis studies on NOMA, the fixed power coefficients are assumed for simplicity. For example, in [10], a user scheduling scheme was investigated to achieve full diversity and scheduling fairness. With fixed power coefficients assumed, outage probabilities were derived in closed-from expressions. In [7], the achievable delay-guaranteed secrecy rate was studied for a downlink NOMA network with two eavesdropping scenarios: 1) an internal eavesdropper in a purely antagonistic network; and 2) an external eavesdropper in a trustworthy network. In [19], with fixed power coefficients considered, the performance of adaptive modulation was investigated for a two-user NOMA network with a family of M-QAM modulations. It was found that at high signal-to-noise ratios (SNRs), the strong user's modulation order converges to the highest order the system can support, but the weak user's constellation size is bounded by the BER requirement and the ratio of power coefficients of the users. Further, it was shown that with the fixed power coefficients, the uncoded M-QAM modulation has an effective power loss of $K$ relative to Shannon rate, where $K$ is a function of BER requirement.

Although fixed power coefficients are commonly used in performance analysis studies, it is still critical to study the performance of joint adaptive transmission including both adaptive modulation and power adaptation strategies. Without sacrificing BER, joint adaptive transmission can improve spectrum efficiency by fully utilizing the time-varying nature of wireless channels, which allows to transmit data at high rate under favorable channel conditions and to reduce rate under poor channel conditions [18]. It is, however, challenging to investigate the performance of joint adaptive transmission that allows both power and rate to adapt to channel fading. In this paper, the main focus is on practical adaptive M-QAM modulation and power adaptation strategies for a downlink two-user NOMA network in which the average SEs will be studied while guaranteeing minimum target rates and BER requirements. We consider a downlink transmission where a base station transmits the superimposed signals to both users. According to [18], with a family of M-QAM modulations, the BER for a Rayleigh fading channel is bounded by a function of constellation size and received SNR. This indicates that for each user, the maximum constellation size for a given BER requirement can be found, which is a function of received SNR. We first propose two adaptive power allocation strategies, each of which guarantees the minimum target rate for one user while providing the highest possible rate for the other. Then, joint adaptive transmission including the two power adaptation strategies and adaptive modulation is studied. Based on the proposed power schemes, a dynamic rate and power adaptation algorithm is also proposed with the aim to further push up the total rate. Note that the considered two-user model can be extended to multiple NOMA clusters by performing user pairing, where each cluster is composed of two users. By allocating orthogonal frequency bands to different NOMA clusters, each NOMA pair can be managed independently. The main contributions of this article are summarized below.

- Two adaptive power strategies are proposed for a downlink two-user NOMA network, i.e., *Scheme 1* and *Scheme 2*. *Scheme 1* aims to guarantee the minimum target rate for the strong user while the weak user maintaining a transmission rate as high as possible. Meanwhile, *Scheme 2* guarantees the minimum target rate for the weak user while providing the highest possible rate for the strong user.
- Consider adaptive continuous-rate modulation where the constellation size continuously adapts to channel fading. It is proved that for the strong user in *Scheme 1* and the weak user in *Scheme 2*, their average SEs converge to the minimum target rates, while the average SEs for the weak user in *Scheme 1* and the strong user in *Scheme 2* are unbounded and monotonically increase with transmit SNR.
- Considering practical discrete-rate M-QAM modulation where the constellation sizes are restricted to integer values, the joint adaptive transmission including both discrete-rate modulation and power adaptation schemes are studied. It is proved that for the strong user in *Scheme 1* and the weak user in *Scheme 2*, their average SEs converge to the minimum target rates. For the weak user in *Scheme 1* and the strong user in *Scheme 2*, their constellation sizes are bounded by the highest modulation order in the system.
- Finally, a dynamic rate and power adaptation (DRPA) algorithm is proposed with the aim to further increase the rate of one user without sacrificing the rate of the other. The Pseudocode of DRPA is illustrated in Algorithm 1. Simulations show that at high SNRs, for the strong user in *Scheme 1* and the weak user in *Scheme 2*, the adoption of DRPA allows the average SEs continue to increase until they reach the highest transmission rate the system can support. The percentage increase in average SE for each user at high SNRs due to the adoption of DRPA can be quantified.

The remainder of this paper is organized as follows.

System model is introduced in Section II. In Section III, we analyze the average SEs for the joint adaptive transmission including both power adaptation and adaptive M-QAM modulations for a downlink two-user NOMA network. The DRPA algorithm is also proposed in Section III. Simulation results are included in Section IV, followed by conclusions summarized in Section V.

## II. System Model

In this paper, a downlink transmission is considered where a base station (BS) transmits signals to two NOMA users. The wireless channels from the BS to NOMA users are assumed to be block fading, i.e., the channel gains remain constant within each fading-block and independently vary from one block to the next. Each fading-block duration $T_f$ is equal to the frame size, which is an integer multiple of the symbol period. Rayleigh fading is considered to reflect the channel variations due to the constructive and destructive addition of multipath signal components [20]. Without any loss of generality, the time-varying channel gains are assumed to be stationary and ergodic. Moreoever, it is assumed that $\sqrt{g_1(i)} > \sqrt{g_2(i)^2}$, where $\sqrt{g_1(i)}$ and $\sqrt{g_2(i)}$ represent the channel gains of user 1 and user 2 at time $i$, respectively. The user with a higher channel gain, i.e., user 1, is called the strong user, while user 2 is called the weak user in this article. The BS transmits the superimposed signal to both users, where the allocated power coefficients for NOMA users can be fixed or adaptive. With fixed power coefficients considered, the BS transmits the signal $\sum_{m=1}^{2} \sqrt{a_m P} s_m$ to both users, where $a_m$ is the power coefficient for user $m$, $P$ is the total transmission power, and $s_m$ is the message for the user $m$. According to NOMA principle, the users' power coefficients should satisfy $\sum_{m=1}^{2} a_m = 1$, and $0 < a_1 < a_2 < 1$. We consider a family of M-QAM constellations with a fixed symbol rate $T_\mathrm{s}$, where $M$ denotes the constellation size. Ideal Nyquist transmission symbol rate is assumed to be satisfied, i.e., $T_\mathrm{s} = 1/B$, where $B$ refers to the bandwidth. Then, the spectral efficiency equals $\log_2(M)$ for a given constellation size $M$ [18]. According to [18], the BER for a fading channel with M-QAM is related to the constellation size. The BER for Rayleigh fading channel with M-QAM modulation is bounded by

$$\mathrm{BER} \leq \int 2e^{-1.5\gamma/(M-1)} f(\gamma) d\gamma, \tag{1}$$

where $f(\gamma)$ indicates the probability density function (PDF) of the received SNR $\gamma$. From (1), it can be noticed that we can adjust constellation size $M$ to maintain a required BER.

[2]Please note that the two users' channel conditions can be different when they locate at very different distances from the BS. In this paper, to simplify the analysis, we assume a uniform distance for both users but their channel gains satisfy $\sqrt{g_1(i)} > \sqrt{g_2(i)}$. The time index $i$ will be omitted because the channel gains are assumed to be stationary and ergodic.

## III. Joint Adaptive Modulation and Power Adaptation

In this section, we study the joint adaptive transmission including both adaptive modulation and power adaptation for a downlink two-user NOMA network. Firstly, we propose two adaptive power allocation strategies in Section III-A. Then, based on the adaptive power schemes, the performance of adaptive continuous-rate modulation in terms of average SEs is analyzed in Section III-B, followed by the analysis of average SEs for adaptive discrete-rate modulation in Section III-C. Finally, we propose a dynamic rate and power adaptation algorithm in Section III-D.

### A. Adaptive Power Allocation Strategies

In order to apply adaptive power allocation strategies, the BS needs to know the perfect channel state information (CSI) of forward links. The BS first sends known pilot signals to both users on the forward link. We assume that each user can get the perfect estimate of forward link CSI and then feedback the obtained CSI estimation to the BS without delay [21]. It is also assumed that the feedback path does not introduce any errors [20]. Since we consider that NOMA users' power coefficients can adapt to the channel fading, they can be written as $a_1(g_1, g_2)$ and $a_2(g_1, g_2)$, respectively. According to NOMA principle, the two users' power coefficients should satisfy $\sum_{m=1}^{2} a_m(g_1, g_2) = 1$ and $0 < a_1(g_1, g_2) < a_2(g_1, g_2) < 1$. The received signals at both users are corrupted by additive white Gaussian noise. Therefore, the instantaneous received SNRs at time $i$ can be expressed as

$$\gamma_1(i) = \gamma_\mathrm{t} a_1(g_1, g_2) g_1(i), \tag{2a}$$

$$\gamma_2(i) = \frac{\gamma_\mathrm{t} a_2(g_1, g_2) g_2(i)}{1 + \gamma_\mathrm{t} a_1(g_1, g_2) g_2(i)}, \tag{2b}$$

where $\gamma_\mathrm{t}$ is the total transmit SNR, i.e., $\gamma_\mathrm{t} = P/N_0 B$, and $N_0$ denotes the noise density.

As mentioned in Section II, the BER for a Rayleigh fading channel with M-QAM modulation is bounded by the constellation size. Hence, in order to guarantee

a required BER, the constellation size is bounded. By rearranging (1) and applying the received SNRs given in (2a) and (2b), the maximum constellation size for a given BER can be given by

$$M_1(g_1,g_2) = 1 + \frac{-1.5}{\ln(0.5\text{BER})}\gamma_\text{t} a_1(g_1,g_2)g_1, \quad (3a)$$

$$M_2(g_1,g_2) = 1 + \frac{-1.5}{\ln(0.5\text{BER})}\frac{\gamma_\text{t} a_2(g_1,g_2)g_2}{1+\gamma_\text{t} a_1(g_1,g_2)g_2}, \quad (3b)$$

where $M_1(g_1,g_2)$ and $M_2(g_1,g_2)$ are the maximum constellation size satisfying the BER requirements for the strong user and the weak user, respectively. Then, the instantaneous SEs for both users, in b/s/Hz, can be respectively expressed as

$$\begin{aligned} R_1(g_1,g_2) &= \log_2(M_1(g_1,g_2)) \\ &= \log_2\left(1+K\gamma_\text{t} a_1(g_1,g_2)g_1\right), \end{aligned} \quad (4a)$$

$$\begin{aligned} R_2(g_1,g_2) &= \log_2(M_2(g_1,g_2)) \\ &= \log_2\left(1+K\frac{\gamma_\text{t} a_2(g_1,g_2)g_2}{1+\gamma_\text{t} a_1(g_1,g_2)g_2}\right), \end{aligned} \quad (4b)$$

where $K = \frac{-1.5}{\ln(0.5\text{BER})}$.

By applying the SIC technique, the strong user, i.e., User 1, first decodes the weak user's message and eliminates it before decoding its own message. In order to guarantee successful SIC at the strong user, it is required that $R_{2\to1}(g_1,g_2) \geq \hat{R}_2$, where $R_{2\to1}(g_1,g_2)$ is the rate for the strong user to detect the weak user's message and $\hat{R}_2$ is the target rate for User 2 [22]. Otherwise, the strong user cannot correctly decode the weak user's message to remove interference. Also, each user's transmitting rate needs to be larger than or equal to the minimum required rate, i.e., $R_m(g_1,g_2) \geq \hat{R}_m$, $m = 1, 2$. This guarantees that each user can successfully decode their own messages. The above rate requirements need to be all satisfied, otherwise outage may happen. We note that $R_{2\to1}(g_1,g_2)$ can be given by

$$R_{2\to1}(g_1,g_2) = \log_2\left(1+K\frac{\gamma_\text{t} a_2(g_1,g_2)g_1}{1+\gamma_\text{t} a_1(g_1,g_2)g_1}\right). \quad (5)$$

Since we have $g_1 > g_2$, by comparing (4b) with (5), we can find that $R_{2\to1}(g_1,g_2) > R_2(g_1,g_2)$. Therefore, it indicates that if $R_2(g_1,g_2) \geq \hat{R}_2$ is met, the requirement $R_{2\to1}(g_1,g_2) > \hat{R}_2$ is also satisfied. We now list below all the requirements on rate, power coefficient and channel gain.

$$0 < a_1(g_1,g_2) < a_2(g_1,g_2) < 1, \quad (6a)$$

$$a_1(g_1,g_2) + a_2(g_1,g_2) = 1, \quad (6b)$$

$$R_1(g_1,g_2) \geq \hat{R}_1, \quad (6c)$$

$$R_2(g_1,g_2) \geq \hat{R}_2, \quad (6d)$$

$$g_1 \geq g_2. \quad (6e)$$

We set $\theta_1 = 2^{\hat{R}_1}, \theta_2 = 2^{\hat{R}_2}$ where $\theta_1 > 1$ and $\theta_2 > 1$. Then, (6c) and (6d) can be rewritten as

$$\theta_1 \leq M(g_1,g_2) = 1 + K\gamma_\text{t} a_1(g_1,g_2)g_1, \quad (7a)$$

$$\theta_2 \leq M(g_1,g_2) = 1 + K\frac{\gamma_\text{t} a_2(g_1,g_2)g_2}{1+\gamma_\text{t} a_1(g_1,g_2)g_2}. \quad (7b)$$

Since power coefficients are adaptive to the channel gains, the above inequalities can be rewritten to get the lower bounds of power coefficients:

$$a_1(g_1,g_2) \geq \frac{\theta_1 - 1}{K\gamma_\text{t} g_1}, \quad (8a)$$

$$a_2(g_1,g_2) \geq \frac{\theta_2 + \theta_2\gamma_\text{t} g_2 - 1 - \gamma_\text{t} g_2}{(\theta_2 + K - 1)\gamma_\text{t} g_2}, \quad (8b)$$

where (8b) is obtained by replacing $a_1(g_1,g_2)$ in (7b) with $(1 - a_2(g_1,g_2))$. Then, by considering the power coefficient constraint (6b), we can get the upper bound of each power coefficient:

$$a_1(g_1,g_2) \leq \frac{K\gamma_\text{t} g_2 - \theta_2 + 1}{(\theta_2 - 1 + K)\gamma_\text{t} g_2}, \quad (9a)$$

$$a_2(g_1,g_2) \leq \frac{K\gamma_\text{t} g_1 - \theta_1 + 1}{K\gamma_\text{t} g_1}. \quad (9b)$$

We can then define the four boundary values in (8a)-(9b) as follows:

$$a_{1\text{low}}(g_1) = \frac{\theta_1 - 1}{K\gamma_\text{t} g_1}, \quad (10a)$$

$$a_{1\text{upper}}(g_2) = \frac{K\gamma_\text{t} g_2 - \theta_2 + 1}{(\theta_2 - 1 + K)\gamma_\text{t} g_2}, \quad (10b)$$

$$a_{2\text{low}}(g_2) = \frac{\theta_2 + \theta_2\gamma_\text{t} g_2 - 1 - \gamma_\text{t} g_2}{(\theta_2 + K - 1)\gamma_\text{t} g_2}, \quad (10c)$$

$$a_{2\text{upper}}(g_1) = \frac{K\gamma_\text{t} g_1 - \theta_1 + 1}{K\gamma_\text{t} g_1}. \quad (10d)$$

From the above analysis, it is clear the two power coefficients satisfy $a_{1\text{low}}(g_1) \leq a_1(g_1,g_2) \leq a_{1\text{upper}}(g_2)$ and $a_{2\text{low}}(g_2) \leq a_2(g_1,g_2) \leq a_{2\text{upper}}(g_1)$. Also, it is easy to find that $a_{1\text{low}}(g_1) + a_{2\text{upper}}(g_1) = 1$ and $a_{1\text{upper}}(g_2) + a_{2\text{low}}(g_2) = 1$. Hence, we obtain two adaptive power coefficient schemes. *Scheme 1*, in which $a_{1\text{low}}(g_1), a_{2\text{upper}}(g_1)$ are chosen as coefficients, guarantees that the strong user stays at the minimum target rate while the weak user has a transmit rate as high as

possible. *Scheme 2* uses $a_{1\text{upper}}(g_2), a_{2\text{low}}(g_2)$ as power coefficients to guarantee the minimum required rate for the weak user while providing the highest possible rate for the strong user. To make *Scheme 1* and *Scheme 2* applicable, (6a)-(6e) all need to be satisfied. Hence, we need to find the necessary conditions that guarantee the rate, power and channel gain requirements for *Scheme 1* and *Scheme 2*.

*1) Scheme 1:*

Let us first focus on *Scheme 1* and list all the required constraints below.

$$0 < a_{1\text{low}}(g_1) < a_{2\text{upper}}(g_1) < 1, \tag{11a}$$
$$a_{1\text{low}}(g_1) + a_{2\text{upper}}(g_1) = 1, \tag{11b}$$
$$R_1(g_1, g_2) \mid_{a_{1\text{low}}(g_1)} \geq \hat{R}_1, \tag{11c}$$
$$R_2(g_1, g_2) \mid_{a_{2\text{upper}}(g_1)} \geq \hat{R}_2, \tag{11d}$$
$$g_1 \geq g_2. \tag{11e}$$

Apparently, (11b) and (11c) are already satisfied. By inserting (10a) and (10d) into (11a), we can get that

$$0 < \frac{\theta_1 - 1}{K\gamma_\text{t} g_1} < \frac{K\gamma_\text{t} g_1 - \theta_1 + 1}{K\gamma_\text{t} g_1} < 1, \tag{12}$$

which indicates that the following constraint needs to be satisfied:

$$g_1 > \frac{2\theta_1 - 2}{K\gamma_\text{t}}. \tag{13}$$

Then, in order to satisfy (11d), we have that

$$\theta_2 \leq 1 + K\frac{\gamma_\text{t} a_{2\text{upper}}(g_1) g_2}{1 + \gamma_\text{t}(1 - a_{2\text{upper}}(g_1)) g_2}. \tag{14}$$

By inserting (10d) into (14) and after doing some basic algebraic operations, we get that

$$(K\gamma_\text{t} g_1 - \theta_1 + 1) K g_1 \geq g_2(\theta_1 - 1)(K + \theta_2 - 1). \tag{15}$$

From (12), we know that $K\gamma_\text{t} g_1 - \theta_1 + 1 > 0$ is definitely guaranteed. Hence, we get that in order to satisfy (11d), the following constraint needs to be satisfied:

$$g_1 \geq \frac{g_2(\theta_2 - 1 + K)(\theta_1 - 1)}{K(K\gamma_\text{t} g_2 - \theta_2 + 1)}. \tag{16}$$

Since now we have two lower bounds of $g_1$, i.e., (13) and (16), we need to find the tighter one. Let us assume that $\frac{2\theta_1 - 2}{K\gamma_\text{t}} < \frac{g_2(\theta_2 - 1 + K)(\theta_1 - 1)}{K(K\gamma_\text{t} g_2 - \theta_2 + 1)}$. Then, this means that $(K - \theta_2 + 1)\gamma_\text{t} g_2 < 2\theta_2 - 2$. When the BER requirement is $10^{-3}$, $K \approx 0.2$. Hence, it is acceptable to assume that $\theta_2 > K + 1$. Then, it can be noted that the constraint is definitely satisfied: $(K - \theta_2 + 1)\gamma_\text{t} g_2 < 2\theta_2 - 2$. Therefore, we can find that (16) is a tighter bound. Finally, we can conclude that for *Scheme 1*, the required constraints on rate, power and channel gain, i.e., (11a)-(11e), can be all guaranteed by just satisfying the two constraints: (11e) and (16).

*2) Scheme 2*

Now let us focus on *Scheme 2* and list all the required constraints below.

$$0 < a_{1\text{upper}}(g_2) < a_{2\text{low}}(g_2) < 1, \tag{17a}$$
$$a_{1\text{upper}}(g_2) + a_{2\text{low}}(g_2) = 1, \tag{17b}$$
$$R_1(g_1, g_2) \mid_{a_{1\text{upper}}(g_2)} \geq \hat{R}_1, \tag{17c}$$
$$R_2(g_1, g_2) \mid_{a_{2\text{low}}(g_2)} \geq \hat{R}_2, \tag{17d}$$
$$g_1 \geq g_2. \tag{17e}$$

Similarly, (17b) and (17d) are already satisfied. By inserting (10b) and (10c) into (17a), we get that

$$0 < \frac{K\gamma_\text{t} g_2 - \theta_2 + 1}{(\theta_2 - 1 + K)\gamma_\text{t} g_2} < \frac{\theta_2 + \theta_2\gamma_\text{t} g_2 - 1 - \gamma_\text{t} g_2}{(\theta_2 + K - 1)\gamma_\text{t} g_2} < 1. \tag{18}$$

By assuming that $\theta_2 > K + 1$, we have that

$$g_2 > \frac{\theta_2 - 1}{K\gamma_\text{t}}. \tag{19}$$

Then, in order to guarantee (17c), we have that

$$\theta_1 \leq 1 + K\gamma_\text{t} a_{1\text{upper}}(g_2) g_1. \tag{20}$$

By inserting (10b) and after doing some basic algebraic operations, we end up with (16). Hence, we can conclude that for *Scheme 2*, in order to guarantee all the required constraints on rate, power and channel gain, i.e., (17a)-(17e), the two constraints, (17e) and (16), need to be satisfied.

*3) Necessary Conditions for Scheme 1 and Scheme 2*

In the above discussions, we consider *Scheme 1* and *Scheme 2* separately. In order to guarantee that both schemes are applicable, we put all the requirements together as shown below.

$$g_1 \geq \frac{g_2(\theta_2 - 1 + K)(\theta_1 - 1)}{K(K\gamma_\text{t} g_2 - \theta_2 + 1)}, \tag{21a}$$
$$g_1 > g_2, \tag{21b}$$
$$g_2 > \frac{\theta_2 - 1}{K\gamma_\text{t}}. \tag{21c}$$

Note that there are two lower bounds of $g_1$. In order to further investigate the ranges of $g_1$ and $g_2$, let us first assume that

$$\frac{g_2(\theta_2 - 1 + K)(\theta_1 - 1)}{K(K\gamma_\text{t} g_2 - \theta_2 + 1)} > g_2. \tag{22}$$

Since (21c) guarantees that $K\gamma_{\mathrm{t}}g_2 - \theta_2 + 1 > 0$, rewritting (22) shows that

$$g_2 < \frac{(\theta_2 - 1 + k)(\theta_1 - 1) + K(\theta_2 - 1)}{K^2\gamma_{\mathrm{t}}}. \tag{23}$$

Furthermore, we can easily obtain that $\frac{(\theta_2-1+k)(\theta_1-1)+K(\theta_2-1)}{K^2\gamma_{\mathrm{t}}} > \frac{\theta_2-1}{K\gamma_{\mathrm{t}}}$.

***Lemma 1:*** In order to guarantee the minimum rate requirements and power coefficients constraints for *Scheme 1* and *Scheme 2*, the following necessary conditions need to be satisfied:

(i) When $\frac{\theta_2-1}{K\gamma_{\mathrm{t}}} < g_2 < \frac{(\theta_2-1+k)(\theta_1-1)+K(\theta_2-1)}{K^2\gamma_{\mathrm{t}}}$, the lower bound of $g_1$ is

$$g_1 > \frac{g_2(\theta_2 - 1 + K)(\theta_1 - 1)}{K(K\gamma_{\mathrm{t}}g_2 - \theta_2 + 1)}. \tag{24}$$

(ii) When $g_2 \geq \frac{(\theta_2-1+k)(\theta_1-1)+K(\theta_2-1)}{K^2\gamma_{\mathrm{t}}}$, the lower bound of $g_1$ is

$$g_1 > g_2. \tag{25}$$

*Proof:* The proof follows the above discussions and is omitted here. ■

### B. Performance of Continuous-Rate Modulation

In this subsection, we consider that we can benefit from exploiting continuous-rate modulation. In other words, we place no restrictions on the constellation sizes, i.e., $M_1(g_1, g_2)$ and $M_2(g_1, g_2)$, where the sizes are not restricted to integer values. Thus, the instantaneous SE, varying with the constellation size, in turn continuously varies with the instantaneous channel gain. We analyze the average SEs for the downlink two-user NOMA network with joint adaptive transmission including adaptive power strategies and continuous-rate modulations.

The average SEs for the strong user and the weak user can be respectively expressed as (26a) and (26b), shown at the top of the next page. where $E[\cdot]$ indicates the expectation and $f_{(1)(2)}(g_1, g_2)$ is the joint PDF of $g_1$ and $g_2$. Since the channel gains of the two users are ordered, the theory of order statistics needs to be used to obtain the joint PDF [23]. For the unordered independent channel gains that are Rayligh distributed with a unit variance, the PDF $f(g)$ and the cumulative distribution function (CDF) $F(g)$ are respectively given by $f(g) = e^{-g}$, $F(g) = 1 - e^{-g}$. According to [23], we can get that $f_{(1)(2)}(g_1, g_2) = 2e^{-g_1}e^{-g_2}$. Hence, we provide the following theorem.

***Theorem 1:*** Consider adaptive continuous-rate M-QAM modulation and adaptive power coefficients. For *Scheme 1*, the average SEs for the strong user and the weak user are respectively given by (27a) and (27b) shown at the top of the next page, where $l_1 = \frac{\theta_2-1}{K\gamma_{\mathrm{t}}}$, $l_2 = \frac{(\theta_2-1+K)(\theta_1-1)+K(\theta_2-1)}{K^2\gamma_{\mathrm{t}}}$, $l_3 = \frac{g_2(\theta_2-1+K)(\theta_1-1)}{K(K\gamma_{\mathrm{t}}g_2-\theta_2+1)}$, and $l_4 = g_2$. For *Scheme 2*, the average SEs for the strong user and the weak user are respectively given by (28a) and (28b) shown at the top of the next page, where $t = \frac{K(K\gamma_{\mathrm{t}}g_2-\theta_2+1)}{(\theta_2-1+K)g_2}$.

*Proof:* See Appendix A. ■

The accuracy of the above analytical results will be validated in Section IV. We also provide the following Lemma 2 which provides the limits as the transmit SNR approaches infinity.

***Lemma 2:*** Consider adaptive continuous-rate M-QAM modulation and adaptive power coefficients. For *Scheme 1*, when transmit SNR $\gamma_{\mathrm{t}} \to \infty$, $\lim_{\gamma_{\mathrm{t}}\to\infty} \bar{R}_1 = \log_2(\theta_1)$, $\lim_{\gamma_{\mathrm{t}}\to\infty} \bar{R}_2 \to \infty$. For *Scheme 2*, when transmit SNR $\gamma_{\mathrm{t}} \to \infty$, $\lim_{\gamma_{\mathrm{t}}\to\infty} \bar{R}_1 \to \infty$, $\lim_{\gamma_{\mathrm{t}}\to\infty} \bar{R}_2 = \log_2(\theta_2)$.

*Proof:* See Appendix B. ■

Lemma 2 proves that the average SE for the strong user in *Scheme 1* and that for the weak user in *Scheme 2* converge to the minimum target rates, when adaptive continuous-rate M-QAM modulation and adaptive power coefficients are considered. On the other hand, for the weak user in *Scheme 1* and the strong user in *Scheme 2*, their average SEs are unbounded and monotonically increase with transmit SNR.

### C. Performance of Adaptive Discrete-Rate Modulation

In Section III-B, adaptive continuous-rate modulation is considered, where the modulation method continuously adapts to the channel fading. However, in practice, the modulation technique in cellular networks works in discrete rate and the constellation sizes are restricted to integer values. In this subsection, we consider adaptive discrete-rate modulation for the downlink two-user NOMA network with a family of M-QAM modulations.

M-QAM constellation sizes are represented by $M_0 = 0, M_1 = 2$ and $M_j = 2^{2(j-1)}$, $j = 2, \ldots, N$. Specifically, $M_0$ indicates the deep fading channel that no data is transmitted and $M_N$ refers to the maximum modulation order in the communication system [20]. At each symbol time, a constellation from the set $\{M_j : j = 0, 1, \ldots, N\}$ is transmitted, where the choice of constellation depends on the fade level over that symbol period [18]. More specifically, the constellation size associated with an instantaneous fading level is determined by discretizing the range of channel fade levels. For each user, the range of channel gain is divided into $N + 1$ fading regions, where the $j$-th region is associated with the constellation $M_j$. To obtain the constellation size, we need to find $j$ such

$$\bar{R}_1 = \mathrm{E}[\log_2(M_1(g_1,g_2))] = \iint \log_2\left(1 + K\gamma_{\mathrm{t}} a_1(g_1,g_2) g_1\right) f_{(1)(2)}(g_1,g_2)\mathrm{d}g_1\mathrm{d}g_2, \tag{26a}$$

$$\bar{R}_2 = \mathrm{E}[\log_2(M_2(g_1,g_2))] = \iint \log_2\left(1 + K\frac{\gamma_{\mathrm{t}} a_2(g_1,g_2) g_2}{1+\gamma_{\mathrm{t}} a_1(g_1,g_2) g_2}\right) f_{(1)(2)}(g_1,g_2)\mathrm{d}g_1\mathrm{d}g_2, \tag{26b}$$

---

$$\bar{R}_1 = \mathrm{E}[\log_2(\theta_1)] = \int_{l_1}^{l_2} 2e^{-g_2-l_3}\log_2(\theta_1)\mathrm{d}g_2 + \log_2(\theta_1)e^{-2l_2}, \tag{27a}$$

$$\begin{aligned}\bar{R}_2 = &\int_{l_1}^{l_2}\int_{l_3}^{\infty} \log_2\left(1 + K\frac{\gamma_{\mathrm{t}} a_{2\mathrm{upper}}(g_1) g_2}{1+\gamma_{\mathrm{t}} a_{1\mathrm{low}}(g_1) g_2}\right) 2e^{-g_1}e^{-g_2}\mathrm{d}g_1\mathrm{d}g_2 \\ &+ \int_{l_2}^{\infty}\int_{l_4}^{\infty} \log_2\left(1 + K\frac{\gamma_{\mathrm{t}} a_{2\mathrm{upper}}(g_1) g_2}{1+\gamma_{\mathrm{t}} a_{1\mathrm{low}}(g_1) g_2}\right) 2e^{-g_1}e^{-g_2}\mathrm{d}g_1\mathrm{d}g_2,\end{aligned} \tag{27b}$$

---

$$\bar{R}_1 = \int_{l_1}^{l_2} 2e^{-g_2}\int_{l_3}^{\infty}\log_2(1+tg_1)e^{-g_1}\mathrm{d}g_1\mathrm{d}g_2 + \int_{l_2}^{\infty} 2e^{-g_2}\int_{l_4}^{\infty}\log_2(1+tg_1)e^{-g_1}\mathrm{d}g_1\mathrm{d}g_2, \tag{28a}$$

$$\bar{R}_2 = \mathrm{E}[\log_2(\theta_2)] = \int_{l_1}^{l_2} 2e^{-g_2-l_3}\log_2(\theta_2)\mathrm{d}g_2 + \log_2(\theta_2)e^{-2l_2}, \tag{28b}$$

---

that $\log_2(M_j) \le R_i < \log_2(M_{j+1})$, $j = 0, 1, \ldots, N$, $i = 1, 2$. Thus, for an instantaneous fade level, the largest constellation in the set $\{M_j : j = 0, 1, \ldots, N\}$ that is smaller than $2^{R_i}$ is transmitted. For the constellation $M_j > 0$, the data rate is thus $\log_2 M_j$.

Let us consider *Scheme 1* first. Note that in *Scheme 1*, the strong user is kept at the minimum required rate $\hat{R}_1$. Its constellation size is also fixed, which equals $\theta_1$. Thus, the average SE for the strong user in *Scheme 1* is $\mathrm{E}[\log_2(\theta_1)]$ or $\mathrm{E}[\hat{R}_1]$. Similar to Theorem 1, with the necessary conditions given in Lemma 1 considered, the analytical expression for $\bar{R}_1$ in *Scheme 1* will be given in Theorem 2. Then, we only need to investigate the average SE for the weak user. For the weak user in *Scheme 1*, the rule of selecting constellation size $M_j$ is

$$M_j \le 1 + K\frac{\gamma_{\mathrm{t}} a_{2\mathrm{upper}}(g_1) g_2}{1+\gamma_{\mathrm{t}}(1-a_{2\mathrm{upper}}(g_1)) g_2} < M_{j+1}. \tag{29}$$

Let us first consider the lower bound. By rewriting this inequality, we get that

$$a_{2\mathrm{upper}}(g_1) \ge \frac{(M_j-1)(1+\gamma_{\mathrm{t}} g_2)}{\gamma_{\mathrm{t}} g_2 (K+M_j-1)}. \tag{30}$$

By setting $N_j = \frac{(M_j-1)(1+\gamma_{\mathrm{t}} g_2)}{\gamma_{\mathrm{t}} g_2 (K+M_j-1)}$ and inserting $a_{2\mathrm{upper}}(g_1)$ into (30), we find that when $g_2 > \frac{M_j-1}{K\gamma_{\mathrm{t}}}$,

$$g_1 \ge \frac{\theta_1 - 1}{K\gamma_{\mathrm{t}} - N_j K\gamma_{\mathrm{t}}}. \tag{31}$$

Similarly, the upper bound of (29) can be rewritten as

$$a_{2\mathrm{upper}}(g_1) < \frac{(M_{j+1}-1)(1+\gamma_{\mathrm{t}} g_2)}{\gamma_{\mathrm{t}} g_2 (K+M_{j+1}-1)}. \tag{32}$$

By setting $N_{j+1} = \frac{(M_{j+1}-1)(1+\gamma_{\mathrm{t}} g_2)}{\gamma_{\mathrm{t}} g_2 (K+M_{j+1}-1)}$ and inserting $a_{2\mathrm{upper}}(g_1)$ into (32), we find that when $g_2 > \frac{M_{j+1}-1}{K\gamma_{\mathrm{t}}}$, we get that

$$g_1 < \frac{\theta_1 - 1}{K\gamma_{\mathrm{t}} - N_{j+1} K\gamma_{\mathrm{t}}}. \tag{33}$$

On the other hand, when $g_2 < \frac{M_{j+1}-1}{K\gamma_{\mathrm{t}}}$, we get that

$$g_1 > \frac{\theta_1 - 1}{K\gamma_{\mathrm{t}} - N_{j+1} K\gamma_{\mathrm{t}}}. \tag{34}$$

We now jointly consider the lower bound and upper bound of (29). As can be noticed from the discussions, the lower bound of (29) is now converted into (31), while the upper bound of (29) is now transformed into (33) and (34). Combining (31) with (33) yields that when $g_2 > \frac{M_{j+1}-1}{K\gamma_{\mathrm{t}}}$, then $\frac{\theta_1-1}{K\gamma_{\mathrm{t}}-N_j K\gamma_{\mathrm{t}}} \le g_1 < \frac{\theta_1-1}{K\gamma_{\mathrm{t}}-N_{j+1}K\gamma_{\mathrm{t}}}$. Combining (31) with (34) implies that when $\frac{M_j-1}{K\gamma_{\mathrm{t}}} < g_2 < \frac{M_{j+1}-1}{K\gamma_{\mathrm{t}}}$, the inequality $g_1 \ge \frac{\theta_1-1}{K\gamma_{\mathrm{t}}-N_j K\gamma_{\mathrm{t}}}$ holds. Hence, by inserting $N_j$ and $N_{j+1}$ into the above inequalities, we conclude that the rule of selecting constellation

size $M_j$, i.e., (29), can be finally converted into the following two conditions:

(i) When $g_2 > \frac{M_{j+1}-1}{K\gamma_{\rm t}}$, the following condition must hold.

$$\frac{g_2(K+M_j-1)(\theta_1-1)}{K(K\gamma_{\rm t}g_2-M_j+1)} \leq g_1 < \frac{g_2(K+M_{j+1}-1)(\theta_1-1)}{K(K\gamma_{\rm t}g_2-M_{j+1}+1)}. \quad (35)$$

(ii) When $\frac{M_j-1}{K\gamma_{\rm t}} < g_2 < \frac{M_{j+1}-1}{K\gamma_{\rm t}}$, the following condition must hold.

$$g_1 \geq \frac{g_2(K+M_j-1)(\theta_1-1)}{K(K\gamma_{\rm t}g_2-M_j+1)}. \quad (36)$$

Recall that in order to guarantee all the requirements on rate, power and channel gain, some necessary conditions need to be satisfied, which are summarized in Lemma 1. Therefore, (35) and (36) need to be constrained by the conditions given in Lemma 1. After doing some basic set operations and by assuming[3] $j < N$ and $\theta_1 \geq 2$, we finally conclude that for the weak user in *Scheme 1*, the constellation $M_j$ is chosen if the following conditions are satisfied:

(i) When $\frac{M_{j+1}-1}{K\gamma_{\rm t}} < g_2 < \frac{(K+M_j-1)(\theta_1-1)+K(M_j-1)}{K^2\gamma_{\rm t}}$, we have that

$$\frac{g_2(K+M_j-1)(\theta_1-1)}{K(K\gamma_{\rm t}g_2-M_j+1)} \leq g_1 < \frac{g_2(K+M_{j+1}-1)(\theta_1-1)}{K(K\gamma_{\rm t}g_2-M_{j+1}+1)}. \quad (37)$$

(ii) When $\frac{(K+M_j-1)(\theta_1-1)+K(M_j-1)}{K^2\gamma_{\rm t}} < g_2 < \frac{(K+M_{j+1}-1)(\theta_1-1)+K(M_{j+1}-1)}{K^2\gamma_{\rm t}}$, we have that

$$g_2 < g_1 < \frac{g_2(K+M_{j+1}-1)(\theta_1-1)}{K(K\gamma_{\rm t}g_2-M_{j+1}+1)}. \quad (38)$$

(iii) When $\frac{M_j-1}{K\gamma_{\rm t}} < g_2 < \frac{M_{j+1}-1}{K\gamma_{\rm t}}$, we have that

$$g_1 \geq \frac{g_2(K+M_j-1)(\theta_1-1)}{K(K\gamma_{\rm t}g_2-M_j+1)}. \quad (39)$$

The average SE for the weak user in *Scheme 1* adopting adaptive discrete-rate modulation is defined as the the sum of data rates associated with each fading region multiplied by the probability that channel gain falls into that region [18]. Therefore, when $j < N$, the average SE for the weak user in *Scheme 1* can be written below, based on the above analytical results.

$$\bar{R}_{2j} = \sum_{j=\mu_2}^{N-1} \left(\bar{\Phi}_{1j} + \bar{\Phi}_{2j} + \bar{\Phi}_{3j}\right), \quad (40)$$

[3]The assumption $\theta_1 \geq 2$ is acceptable since it requires that at least BPSK is guaranteed.

where $\bar{\Phi}_{1j}$, $\bar{\Phi}_{2j}$, and $\bar{\Phi}_{3j}$ are respectively given by (41a), (41b), and (41c) shown at the top of the next page. In (40), $\mu_2$ refers to the modulation order related to the minimum required rate $\hat{R}_2$. For example, if the minimum required rate is 1 b/s/Hz, at least BPSK is required, i.e., $\mu_2 = 2$.

The above analysis is valid when $j < N$. The case of $j = N$ needs to be considered separately. It is noted that $M_N = 2^{2(N-1)}$ and $M_{N+1} = \infty$. Hence, for the weak user in *Scheme 1*, the condition of choosing $M_N$ is given by

$$M_N \leq 1 + K\frac{\gamma_{\rm t}a_{2\rm upper}(g_1)g_2}{1+\gamma_{\rm t}(1-a_{2\rm upper}(g_1))g_2} < \infty. \quad (42)$$

After doing some algebraic operations, we can also obtain the ranges of $g_1$ and $g_2$ resulting in the constellation size $M_N$. Similar to the analysis above, we can obtain that when $j = N$, the average SE for the weak user in *Scheme 1* can be given below.

$$\bar{R}_{2N} = \bar{\Phi}_{1N} + \bar{\Phi}_{2N}, \quad (43)$$

where $\bar{\Phi}_{1N}$ and $\bar{\Phi}_{2N}$ are respectively given by (44a) and (44b) shown at the top of the next page. Hence, for both users in *Scheme 1*, we can finally provide the following theorem.

***Theorem** 2:* Consider adaptive discrete-rate M-QAM modulation and adaptive power coefficients. For *Scheme 1*, the average SEs for both users are respectively given by

$$\bar{R}_1 = \mathrm{E}[\log_2(\theta_1)] = \int_{l_1}^{l_2} 2e^{-g_2-l_3}\log_2(\theta_1)\mathrm{d}g_2 + \log_2(\theta_1)e^{-2l_2}, \quad (45a)$$

$$\bar{R}_2 = \bar{R}_{2j} + \bar{R}_{2N} = \sum_{j=\mu_2}^{N-1}\left(\bar{\Phi}_{1j} + \bar{\Phi}_{2j} + \bar{\Phi}_{3j}\right) + \bar{\Phi}_{1N} + \bar{\Phi}_{2N}, \quad (45b)$$

where $l_1 = \frac{\theta_2-1}{K\gamma_{\rm t}}$, $l_2 = \frac{(\theta_2-1+K)(\theta_1-1)+K(\theta_2-1)}{K^2\gamma_{\rm t}}$, and $l_3 = \frac{g_2(\theta_2-1+K)(\theta_1-1)}{K(K\gamma_{\rm t}g_2-\theta_2+1)}$. $\bar{\Phi}_{1j}$, $\bar{\Phi}_{2j}$, $\bar{\Phi}_{3j}$, $\bar{\Phi}_{1N}$, and $\bar{\Phi}_{2N}$ are respectively given in (41a), (41b), (41c), (44a), and (44b).

*Proof:* The proof follows the above analysis. ■

Now let us consider *Scheme 2*. Note that in *Scheme 2*, the weak user remains at the minimum required rate $\hat{R}_2$. Its constellation size is equal to $\theta_2$. Thus, the average SE for the weak user in *Scheme 2* is $\mathrm{E}[\log_2(\theta_2)]$ or $\mathrm{E}[\hat{R}_2]$. With the necessary conditions given in Lemma 1 considered, the analytical expression for $\bar{R}_2$ in *Scheme 2* will be given in Theorem 3. Thus, we only need to

$$\bar{\Phi}_{1j} = \int_{\frac{M_{j+1}-1}{K\gamma_{\rm t}}}^{\frac{(K+M_j-1)(\theta_1-1)+K(M_j-1)}{K^2\gamma_{\rm t}}} \int_{\frac{g_2(K+M_j-1)(\theta_1-1)}{K(K\gamma_{\rm t}g_2-M_j+1)}}^{\frac{g_2(K+M_{j+1}-1)(\theta_1-1)}{K(K\gamma_{\rm t}g_2-M_{j+1}+1)}} \log_2(M_j)\, f_{(1)(2)}(g_1,g_2)\mathrm{d}g_1\mathrm{d}g_2, \tag{41a}$$

$$\bar{\Phi}_{2j} = \int_{\frac{(K+M_j-1)(\theta_1-1)+K(M_j-1)}{K^2\gamma_{\rm t}}}^{\frac{(K+M_{j+1}-1)(\theta_1-1)+K(M_{j+1}-1)}{K^2\gamma_{\rm t}}} \int_{g_2}^{\frac{g_2(K+M_{j+1}-1)(\theta_1-1)}{K(K\gamma_{\rm t}g_2-M_{j+1}+1)}} \log_2(M_j)\, f_{(1)(2)}(g_1,g_2)\mathrm{d}g_1\mathrm{d}g_2, \tag{41b}$$

$$\bar{\Phi}_{3j} = \int_{\frac{M_j-1}{K\gamma_{\rm t}}}^{\frac{M_{j+1}-1}{K\gamma_{\rm t}}} \int_{\frac{g_2(K+M_j-1)(\theta_1-1)}{K(K\gamma_{\rm t}g_2-M_j+1)}}^{\infty} \log_2(M_j)\, f_{(1)(2)}(g_1,g_2)\mathrm{d}g_1\mathrm{d}g_2, \tag{41c}$$

$$\bar{\Phi}_{1N} = \int_{\frac{M_N-1}{K\gamma_{\rm t}}}^{\frac{(K+M_N-1)(\theta_1-1)+K(M_N-1)}{K^2\gamma_{\rm t}}} \int_{\frac{g_2(\theta_1-1)(K+M_N-1)}{K(K\gamma_{\rm t}g_2-M_N+1)}}^{\infty} \log_2(M_N)\, f_{(1)(2)}(g_1,g_2)\mathrm{d}g_1\mathrm{d}g_2, \tag{44a}$$

$$\bar{\Phi}_{2N} = \int_{\frac{(K+M_N-1)(\theta_1-1)+K(M_N-1)}{K^2\gamma_{\rm t}}}^{\infty} \int_{g_2}^{\infty} \log_2(M_N)\, f_{(1)(2)}(g_1,g_2)\mathrm{d}g_1\mathrm{d}g_2. \tag{44b}$$

study the average SE for the strong user. For the strong user in *Scheme 2*, the rule of selecting constellation size $M_j$ is

$$M_j \le 1 + K\gamma_{\rm t} a_{1\rm upper}(g_2) g_1 < M_{j+1}. \tag{46}$$

Similar to the analysis for the weak user in *Scheme 1*, we can obtain that for the strong user in *Scheme 2*, the constellation $M_j$ is chosen if the following condition is satisfied:

(i) When $g_2 > \frac{\theta_2-1}{K\gamma_{\rm t}}$, we have that

$$\frac{g_2(K+\theta_2-1)(M_j-1)}{K(K\gamma_{\rm t}g_2-\theta_2+1)} \le g_1 < \frac{g_2(K+\theta_2-1)(M_{j+1}-1)}{K(K\gamma_{\rm t}g_2-\theta_2+1)}. \tag{47}$$

Recall that Lemma 1 summarizes the necessary conditions for the requirements on rate, power and channel gain. To provide valid analysis, (47) needs to be constrained by the conditions given in Lemma 1. Hence, we can conclude that for the strong user in *Scheme 2*, by assuming $j < N$, the average SE is given by

$$\bar{R}_{1j} = \sum_{j=\mu_1}^{N-1} \left(\bar{\Lambda}_{1j} + \bar{\Lambda}_{2j}\right), \tag{48}$$

where $\bar{\Lambda}_{1j}$ and $\bar{\Lambda}_{2j}$ are respectively given by (49a) and (49b) at the top of the next page. In (48), $\mu_1$ refers to the modulation order related to the minimum required rate $\hat{R}_1$. Then, we consider the case of $j = N$. For the strong user in *Scheme 2*, the condition of choosing $M_N$ is given by

$$M_N \le 1 + K\gamma_{\rm t} a_{1\rm upper}(g_2) g_1 < \infty. \tag{50}$$

By doing similar mathematical operations, we can obtain the ranges of $g_1$ and $g_2$ in which the constellation size $M_N$ will be chosen. Hence, for the case of $j = N$, the average SE for the strong user in *Scheme 2* can be given below.

$$\bar{R}_{1N} = \bar{\Lambda}_{1N} + \bar{\Lambda}_{2N}, \tag{51}$$

where $\bar{\Lambda}_{1N}$ and $\bar{\Lambda}_{2N}$ are respectively given by (52a) and (52b) shown at the top of the next page. Hence, for both users in *Scheme 2*, we can finally provide the following theorem.

***Theorem** 3:* Consider adaptive discrete-rate M-QAM modulation and adaptive power coefficients. For *Scheme 2*, the average SEs for both users are respectively given by

$$\bar{R}_1 = \bar{R}_{1j} + \bar{R}_{1N} = \sum_{j=\mu_1}^{N-1} \left(\bar{\Lambda}_{1j} + \bar{\Lambda}_{2j}\right) + \bar{\Lambda}_{1N} + \bar{\Lambda}_{2N}, \tag{53a}$$

$$\bar{R}_2 = \mathrm{E}[\log_2(\theta_2)] = \int_{l_1}^{l_2} 2e^{-g_2-l_3}\log_2(\theta_2)\mathrm{d}g_2 + \log_2(\theta_2)e^{-2l_2}, \tag{53b}$$

where $l_1 = \frac{\theta_2-1}{K\gamma_{\rm t}}$, $l_2 = \frac{(\theta_2-1+K)(\theta_1-1)+K(\theta_2-1)}{K^2\gamma_{\rm t}}$, and $l_3 = \frac{g_2(\theta_2-1+K)(\theta_1-1)}{K(K\gamma_{\rm t}g_2-\theta_2+1)}$. $\bar{\Lambda}_{1j}$, $\bar{\Lambda}_{2j}$, $\bar{\Lambda}_{1N}$, and $\bar{\Lambda}_{2N}$ are respectively given in (49a), (49b), (52a), and (52b).

*Proof:* The proof follows the above analysis. ■

The accuracy of the above derived analytical results in Theorem 2 and 3 will be confirmed in Section IV, by comparing with Monte Carlo results. We further provide the following Lemma 3 which provides the limits as the transmit SNR approaches infinity.

$$\bar{\Lambda}_{1j} = \int_{\frac{\theta_2-1}{K\gamma_{\rm t}}}^{\frac{(K+\theta_2-1)(M_j-1)+K(\theta_2-1)}{K^2\gamma_{\rm t}}} \int_{\frac{g_2(K+\theta_2-1)(M_j-1)}{K(K\gamma_{\rm t}g_2-\theta_2+1)}}^{\frac{g_2(K+\theta_2-1)(M_{j+1}-1)}{K(K\gamma_{\rm t}g_2-\theta_2+1)}} \log_2\left(M_j\right) f_{(1)(2)}(g_1,g_2)\mathrm{d}g_1\mathrm{d}g_2, \tag{49a}$$

$$\bar{\Lambda}_{2j} = \int_{\frac{(K+\theta_2-1)(M_j-1)+K(\theta_2-1)}{K^2\gamma_{\rm t}}}^{\frac{(K+\theta_2-1)(M_{j+1}-1)+K(\theta_2-1)}{K^2\gamma_{\rm t}}} \int_{g_2}^{\frac{g_2(K+\theta_2-1)(M_{j+1}-1)}{K(K\gamma_{\rm t}g_2-\theta_2+1)}} \log_2\left(M_j\right) f_{(1)(2)}(g_1,g_2)\mathrm{d}g_1\mathrm{d}g_2, \tag{49b}$$

$$\bar{\Lambda}_{1N} = \int_{\frac{\theta_2-1}{K\gamma_{\rm t}}}^{\frac{(K+\theta_2-1)(M_N-1)+K(\theta_2-1)}{K^2\gamma_{\rm t}}} \int_{\frac{g_2(K+\theta_2-1)(M_N-1)}{K(K\gamma_{\rm t}g_2-\theta_2+1)}}^{\infty} \log_2\left(M_N\right) f_{(1)(2)}(g_1,g_2)\mathrm{d}g_1\mathrm{d}g_2, \tag{52a}$$

$$\bar{\Lambda}_{2N} = \int_{\frac{(K+\theta_2-1)(M_N-1)+K(\theta_2-1)}{K^2\gamma_{\rm t}}}^{\infty} \int_{g_2}^{\infty} \log_2(M_N) f_{(1)(2)}(g_1,g_2)\mathrm{d}g_1\mathrm{d}g_2. \tag{52b}$$

***Lemma** 3:* Consider adaptive discrete-rate M-QAM modulation and adaptive power coefficients. For *Scheme 1*, when transmit SNR $\gamma_{\rm t}\to\infty$, $\lim\limits_{\gamma_{\rm t}\to\infty}\bar{R}_1=\log_2\left(\theta_1\right)$, $\lim\limits_{\gamma_{\rm t}\to\infty}\bar{R}_2=\log_2\left(M_N\right)$. For *Scheme 2*, when transmit SNR $\gamma_{\rm t}\to\infty$, $\lim\limits_{\gamma_{\rm t}\to\infty}\bar{R}_1=\log_2\left(M_N\right)$, $\lim\limits_{\gamma_{\rm t}\to\infty}\bar{R}_2=\log_2\left(\theta_2\right)$.

*Proof:* For the strong user in *Scheme 1*, we can first find that when $\gamma_{\rm t}\to\infty$, $l_1\to 0$, $l_2\to 0$, $l_3\to 0$. Therefore, similar to Appendix B, we can get that $\lim\limits_{\gamma_{\rm t}\to\infty}\bar{R}_1=\log_2\left(\theta_1\right)$. For the weak user in *Scheme 1*, we can find that when $\gamma_{\rm t}\to\infty$, $\lim\limits_{\gamma_{\rm t}\to\infty}1+K\frac{\gamma_{\rm t}a_{2\rm upper}(g_1)g_2}{1+\gamma_{\rm t}(1-a_{2\rm upper}(g_1))g_2}\to\infty$. Therefore, in this extreme case, the largest modulation order in the system is chosen, i.e., $\lim\limits_{\gamma_{\rm t}\to\infty}\bar{R}_2=\log_2\left(M_N\right)$. For the strong user in *Scheme 2*, when $\gamma_{\rm t}\to\infty$, $\lim\limits_{\gamma_{\rm t}\to\infty}1+K\gamma_{\rm t}a_{1\rm upper}(g_2)g_1\to\infty$. Therefore, the largest modulation order is chosen, i.e., $\lim\limits_{\gamma_{\rm t}\to\infty}\bar{R}_1=\log_2\left(M_N\right)$. For the weak user in *Scheme 2*, we have that when $\gamma_{\rm t}\to\infty$, $l_1\to 0$, $l_2\to 0$, $l_3\to 0$. By inserting them into the analytical expression of $\bar{R}_2$, we finally get that $\lim\limits_{\gamma_{\rm t}\to\infty}\bar{R}_2=\log_2\left(\theta_2\right)$. ∎

Lemma 3 proves that the average SEs for both users in both power schemes are bounded, when adaptive discrete-rate M-QAM modulation and adaptive power coefficients are considered. This is different from the conclusion given in Lemma 2 for adaptive continuous-rate modulation. It is because when continuous-rate modulation is considered, the constellation size continuously adapts to channel fading and is unbounded, while for the practical discrete-rate modulation, the available constellation sizes are discrete and there exists a highest modulation order, due to system limitations. Lemma 3 also indicates that for the strong user in *Scheme 1* and the weak user in *Scheme 2*, their average SEs converge to the minimum target rates. Meanwhile, for the weak user in *Scheme 1* and the strong user in *Scheme 2*, their constellation sizes are bounded by the highest modulation order the system can support.

### *D. Dynamic Rate and Power Adaptation Algorithm*

In Section III-A, we proposed two adaptive power allocation strategies, i.e., *Scheme 1* and *Scheme 2*. Then, in Section III-C, the joint adaptive transmission including both discrete rate and power adaptation was studied for both power allocation schemes. In this section, we propose a dynamic rate and power adaptation scheme, which is based on the two power schemes proposed in III-A but aims to further increase the rate of one user without sacrificing the rate of the other.

The total average SE is $\bar{R}_1+\bar{R}_2$, which equals $\mathrm{E}[\log_2(M_1(g_1,g_2))]+\mathrm{E}[\log_2(M_2(g_1,g_2))]$ where $M_1(g_1,g_2)$ and $M_2(g_1,g_2)$ are the constellations chosen from the set $\{M_j: j=0,1,\ldots,N\}$. Recall that in *Scheme 1*, $a_{1\rm low}(g_1)$ and $a_{2\rm upper}(g_1)$ are the adaptive power coefficients for the strong user and the weak user, respectively. In *Scheme 1*, the total average SE is $\hat{R}_1+\bar{R}_2$, which means the strong user always remains at the minimum target rate $\hat{R}_1$. Hence, we cannot decrease $a_{1\rm low}(g_1)$ because it will violate the rate constraint. However, we can decrease the power coefficient of weak user which in turn increases the power allocation of strong user. Then, the strong user's power coefficient may be large enough to increase its constellation size while the weak user's modulation remains the same. Similarly, in *Scheme 2*, $a_{1\rm upper}(g_2)$ and $a_{2\rm low}(g_2)$ are the adaptive power coefficients, which indicates that $a_{2\rm low}(g_2)$ for the weak user cannot be decreased. However, we can decrease the power

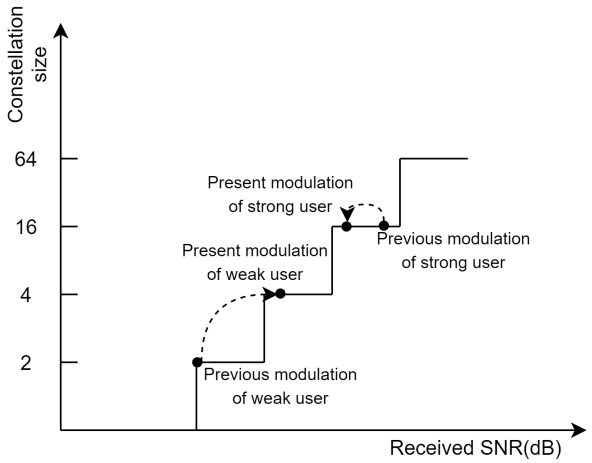

Fig. 1: Principle of DRPA algorithm for *Scheme 2*.

coefficient of strong user in *Scheme 2*, which may leads to a higher modulation order for the weak user, without sacrificing the strong user's rate. To sum up, we aim to carefully adjust the adaptive power coefficients to push up the total average SE further. The principle of DRPA algorithm for *Scheme 2* is given in Fig. 1.

Let us use *Scheme 2* as an example and introduce the DRPA algorithm[4]. But it can also be applied to *Scheme 1*, where the details are explained later. For *Scheme 2*, the current modulation orders for both users are initially known, i.e., $M_1$ and $M_2$, where $M_2$ is related to the minimum target rate. We first decide a new constellation size for the weak user in each iteration, e.g., $M_2^{(n+1)}$, which is the next higher modulation order in the set $\{M_j : j = 0, 1, \ldots, N\}$. Based on the updated $M_2^{(n+1)}$, the new power coefficients for both users can be calculated, as well as the corresponding SEs. Since we aim to push up the weak user's rate without sacrificing the strong user's rate, the loop terminates when the newly updated power coefficients result in a lower SE for the strong user. The final constellation sizes, i.e., $M_1^*$ and $M_2^*$, are obtained respectively. The Pseudocode of DRPA algorithm is illustrated in Algorithm 1.

For *Scheme 1*, the DRPA algorithm shown above needs to be adjusted. Firstly, for *Scheme 1*, we first decide a new constellation size for the strong user in each iteration, e.g., $M_1^{(n+1)}$, which is the next higher modulation order. Then, the power coefficients can be updated using the expressions below. Finally, the loop ends when the weak user's SE is sacrificed.

$$a_1^{(n+1)}(g_1) \leftarrow \frac{M_1^{(n+1)} - 1}{K\gamma_{\mathrm{t}} g_1}, \tag{54a}$$

$$a_2^{(n+1)}(g_1) \leftarrow 1 - a_1^{(n+1)}(g_1). \tag{54b}$$

The effectiveness of the proposed DRPA algorithm will be validated in Section IV.

[4]Since each user has a positive minimum required rate, we omits the case of no data transmission, i.e., choosing constellation $M_0$.

**Algorithm 1** Dynamic Rate and Power Adaptation (DRPA)

**Input:**
$M_1$, $M_2$, $a_{1\mathrm{upper}}(g_2)$, $a_{2\mathrm{low}}(g_2)$, $M_N$
Set iteration index $n = 0$;
Set $M_2^{(0)} \leftarrow M_2$, $R_1^{(0)} \leftarrow \log_2(M_1)$, $a_1^{(0)}(g_2) \leftarrow a_{1\mathrm{upper}}(g_2)$, $a_2^{(0)}(g_2) \leftarrow a_{2\mathrm{low}}(g_2)$;
**while** $a_1^{(n)}(g_2) <= a_2^{(n)}(g_2)$ && $a_2^{(n)}(g_2) < 1$ **do**
  **if** $R_1^{(n)} \geq \log_2(M_1)$ **then**
    $M_2^* \leftarrow M_2^{(n)}$, $a_1^*(g_2) \leftarrow a_1^{(n)}(g_2)$, $a_2^*(g_2) \leftarrow a_2^{(n)}(g_2)$;
  **else**
    Break;
  **end if**
  **if** $M_2^{(n)} = 2$ **then**
    Update $M_2^{(n+1)} \leftarrow 4$;
  **else if** $M_2^{(n)} \geq 4$ **then**
    Update $M_2^{(n+1)} \leftarrow 4M_2^{(n)}$;
  **end if**
  Calculate the new power coefficients in *Scheme 2*: $a_2^{(n+1)}(g_2) \leftarrow \frac{\left(M_2^{(n+1)}-1\right)(1+\gamma_{\mathrm{t}} g_2)}{\left(K+M_2^{(n+1)}-1\right)\gamma_{\mathrm{t}} g_2}$, $a_1^{(n+1)}(g_2) \leftarrow 1 - a_2^{(n+1)}(g_2)$;
  Calculate the corresponding SEs $R_1^{(n+1)}$, $R_2^{(n+1)}$ by inserting $a_2^{(n+1)}(g_2)$, $a_1^{(n+1)}(g_2)$ into (4a) and (4b);
  **if** $M_2^{(n+1)} = M_N$ **then**
    Break;
  **end if**
  Update $n \leftarrow n + 1$;
**end while**
**Output:** $M_1^* \leftarrow M_1$, $M_2^*$, $a_1^*(g_2)$, $a_2^*(g_2)$

## IV. Numerical Results

In this section, the accuracy of the developed analytical results will be validated by comparing with Monte Carlo simulation results. The performance of the proposed DRPA algorithm will also be investigated. The channel gain from BS to each user is assumed to be Raleigh fading with unit variance. The strong user always has larger channel gains than the weak user. The

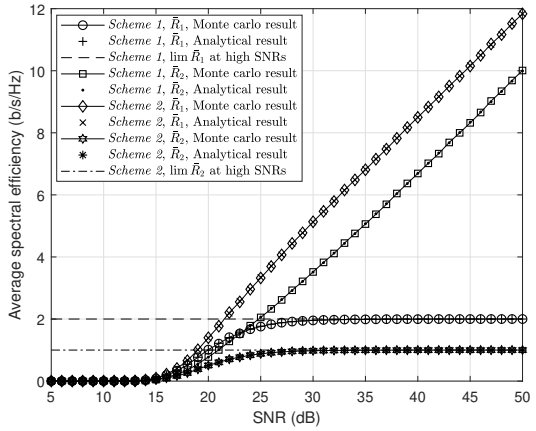


Fig. 2: Average SE versus transmit SNR, with adaptive continuous-rate modulation and power adaptation strategies.

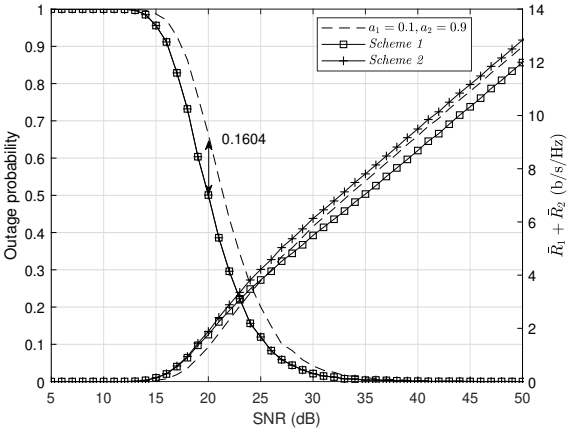


Fig. 3: Outage probability and total average SE versus transmit SNR, with adaptive continuous-rate modulation, power adaptation strategies and fixed power coefficients ($a_1 = 0.1$, $a_2 = 0.9$).

BER requirement is assumed to be $10^{-3}$ for each user, unless otherwise indicated. The choices of constellation size in the system are BPSK, 4-QAM, 16-QAM, 64-QAM, and 256-QAM.

### *A. Adaptive Continuous-Rate Modulation and Power Strategies*

In this subsection, we start to study the performance of adaptive continuous-rate modulation and the two proposed power strategies, via simulations. Fig. 2 is first illustrated showing the average SE versus transmit SNR, in which Monte Carlo results, analytical results and the limits at high SNRs are plotted for *Scheme 1* and *Scheme 2*. The minimum required rates, i.e., $\hat{R}_1$ and $\hat{R}_2$, are set to 2 b/s/Hz and 1 b/s/Hz, respectively. Fig. 2 first shows that the analysis given in Lemma 1 and Theorem 1 are accurate, since the analytical results match well with Monte Carlo simulations. Further, Fig. 2 confirms that when the transmit SNR approaches infinity, the average SE for the strong user in *Scheme 1* converges to the maximum limit $\log_2(\theta_1)$, i.e., $\hat{R}_1$, which equals 2 b/s/Hz according to our parameter settings. On the other hand, Lemma 2 proves that for the weak user in *Scheme 2*, the average SE converges to $\log_2(\theta_2)$, i.e., $\hat{R}_2$. This can be confirmed by Fig. 2. This figure also confirms the other conclusions provided in Lemma 2, i.e., for the weak user in *Scheme 1* and the strong user in *Scheme 2*, their average SEs are unbounded. Lemma 2 is thus fully confirmed.

Fig. 3 is plotted to compare the performance of *Scheme 1*, *Scheme 2* and fixed power coefficients in terms of outage probability and total average SE. According to the guarantees on rate, power and channel gain for the two adaptive power strategies in Section III-A, one can note that the average SEs analyzed in Sections III-B and III-C guarantee the minimum target rate for both users. Hence, to make sure a fair comparison, in Fig. 3, the average SE plotted for the fixed power coefficients is also the achieved average SE with the minimum target rates guaranteed for both users. Fig. 3 shows that when the transmit SNR is smaller than 15 dB, the outage probability is close to 1 for all three approaches, resulting in almost zero b/s/Hz in terms of total average SE. From Fig. 3, one can also notice that the two adaptive power schemes provide much smaller outage probability than the fixed power allocation scheme. For example, when transmit SNR is 20 dB, the outage probability of adaptive power schemes is 16.04% smaller than that of fixed power allocation. It shows that at high SNRs, e.g., $\geq$ 30 dB, *Scheme 2* achieves the highest total SE, while *Scheme 1* obtains the smallest total SE. This can also be confirmed by Fig. 2 since it shows that based on the parameter settings, at high SNRs, the difference between $\bar{R}_1$ in *Scheme 2* and $\bar{R}_2$ in *Scheme 1* is larger than the difference between $\bar{R}_1$ in *Scheme 1* and $\bar{R}_2$ in *Scheme 2*. Fig. 3 also shows that the fixed power allocation with $a_1 = 0.1$ and $a_2 = 0.9$ achieves larger total average SE than *Scheme 1* at high SNRs. But this does not always hold. If the minimum target rates are set to 2 b/s/Hz for both users, we can find that the total average SE for the fixed power allocation with $a_1 = 0.1$ and $a_2 = 0.9$ reduces to zero and the outage probability remains at 1. This means that in this case, this fixed power allocation scheme cannot guarantee the minimum required rates.

On the contrary, the adaptive power strategies, i.e., *Scheme 1* and *Scheme 2*, still provide positive average SEs and outage probability values less than 1.

### *B. Adaptive Discrete-Rate Modulation and Power Strategies*

Then, we investigate the performance of adaptive discrete-rate modulation and power adaptation schemes, i.e., *Scheme 1* and *Scheme 2*. The minimum target rates, i.e., $\hat{R}_1$ and $\hat{R}_2$, are set to 2 b/s/Hz and 1 b/s/Hz. To validate the accuracy of the proposed analytical expressions for $\bar{R}_1$ and $\bar{R}_2$ given in Theorem 2 and Theorem 3, we depict Fig. 4, which plots the average SE versus transmit SNR for both power adaptation schemes. By comparing with Monte Carlo simulations, Fig. 4 confirms that the analytical expressions are accurate. Furthermore, different from Fig. 2 obtained with continuous-rate modulation, Fig. 4 shows that the average SEs achieved with discrete-rate modulation converge to the maximum limits for both users. This is because of the practical system limitations on the modulation order. More details are shown in Fig. 5.

For the discrete-rate modulation, Fig. 5 is plotted to compare the performance of *Scheme 1*, *Scheme 2* and fixed power coefficients with $a_1 = 0.1, a_2 = 0.9$. The minimum required rates, i.e., $\hat{R}_1$ and $\hat{R}_2$, are set to 4 b/s/Hz and 1 b/s/Hz, respectively. Fig. 5 shows that in *Scheme 1*, when the transmit SNR approaches infinity, the average SE for the strong user converges to 4 b/s/Hz, while that of the weak user converges to 8 b/s/Hz. This is because, as proved in Lemma 3, for the strong user in *Scheme 1*, its average SE converges to $\log_2(\theta_1)$ or $\hat{R}_1$. Meanwhile, for the weak user in *Scheme 1*, its average SE converges to $\log_2(M_N)$ where $M_N$ is the highest modulation order, i.e., 256 according to our settings. On the other hand, Fig. 5 also shows that in *Scheme 2*, the average SE for the strong user approaches 8 b/s/Hz, while that of the weak user approaches 1 b/s/Hz, as the transmit SNR increases. This also confirms the proved conclusions in Lemma 3. Furthermore, this figure indicates that $\bar{R}_1$ and $\bar{R}_2$ with $a_1 = 0.1, a_2 = 0.9$ are smaller than that obtained in *Scheme 2*, when the transmit SNR is not very large. However, when the transmit SNR approaches infinity, the average SEs with fixed power coefficients and that in *Scheme 2* converge to the same limits. But this is not always the case. Fig. 6 is plotted where the fixed power coefficients are given by $a_1 = 0.06$ and $a_2 = 0.94$. It is shown that as the transmit SNR approaches infinity, the average SE for the weak user with fixed power coefficients converges to 2 b/s/Hz. This is because, with fixed power coefficients, the

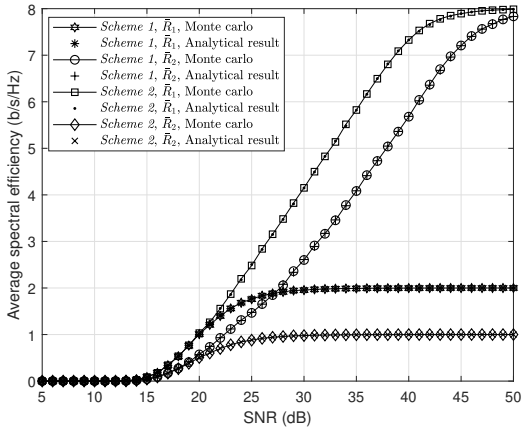


Fig. 4: Average SE versus transmit SNR, with adaptive discrete-rate modulation and power adaptation strategies.

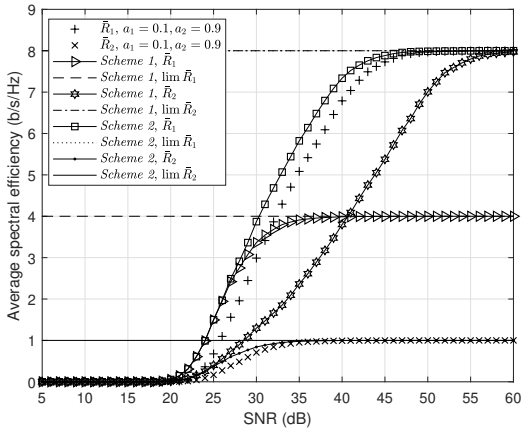


Fig. 5: Average SE versus transmit SNR, with adaptive discrete-rate modulation, power adaptation strategies and fixed power coefficients ($a_1 = 0.1$, $a_2 = 0.9$).

average SE for the weak user at high SNRs is bounded by $\log_2(M_{z_2})$, which is the maximum constellation size that is smaller than $1 + K\frac{a_2}{a_1}$. When the ratio of power coefficients becomes larger, i.e., $a_1 = 0.06, a_2 = 0.94$, we have $1 + K\frac{a_2}{a_1} = 4.0917 > 4$, indicating that for the weak user, 4-QAM is transmitted and the average SE is therefore equal to 2 b/s/Hz. Hence, with fixed power coefficients, the maximum limit of the weak user's average SE is bounded by the BER requirement and the ratio of power coefficients. More details can be found in our previous paper [19].

### *C. Dynamic Rate and Power Adaptation Algorithm*

In this subsection, we check the performance of the DRPA algorithm proposed in Section III-D. The mini-

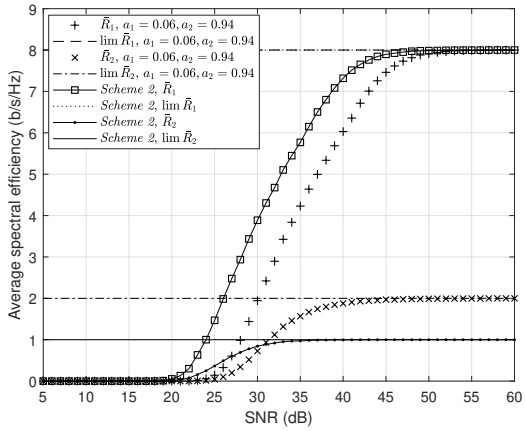


Fig. 6: Average SE versus transmit SNR, with adaptive discrete-rate modulation, power adaptation strategies and fixed power coefficients ($a_1 = 0.06$, $a_2 = 0.94$).

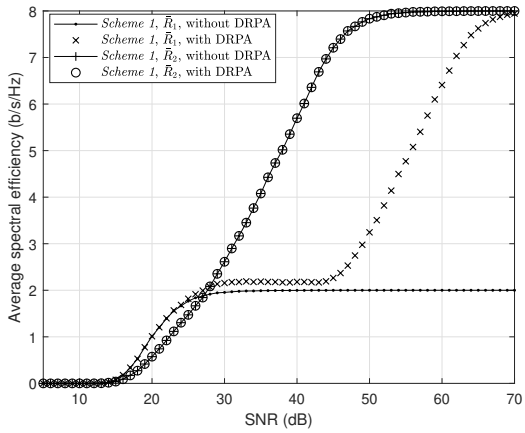


Fig. 7: Average SE versus transmit SNR, for *Scheme 1* with and without DRPA.

mum target rates, i.e., $\hat{R}_1$ and $\hat{R}_2$, are set to 2 b/s/Hz and 1 b/s/Hz, unless otherwise stated. Fig. 7 is first plotted to compare the performance of average SE for *Scheme 1* with and without DRPA algorithm. It is shown that the adoption of DRPA does not change the weak user's average SE in *Scheme 1*. This is because, as discussed in Section III-D, the DRPA algorithm for *Scheme 1* aims to push up the strong user's rate while keeping the weak user's rate unchanged. From Fig. 7, we can easily notice that with DRPA applied, the strong user's average SE in *Scheme 1* is larger than that without DRPA, especially at high SNRs. For example, when the transmit SNR is 70 dB, the average SE achieved with DRPA for the strong user in *Scheme 1* is 4 times larger than that obtained without DRPA. This is because, without

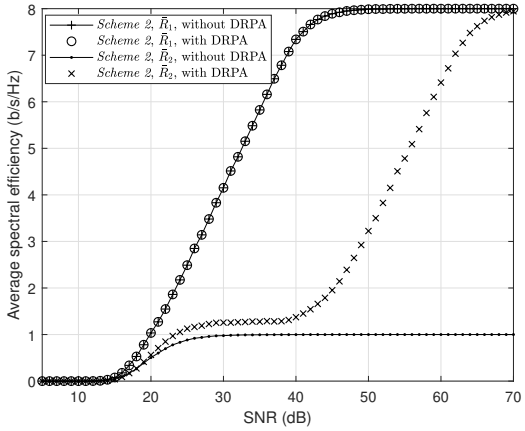


Fig. 8: Average SE versus transmit SNR, for *Scheme 2* with and without DRPA.

DRPA algorithm, $\bar{R}_1$ in *Scheme 1* is bounded by the minimum target rate, i.e., $\hat{R}_1$ or $\log_2(\theta_1)$. However, with DRPA applied, the strong user's average SE continues to increase until its modulation order reaches the maximum limit in the system, i.e., $M_N$. In other words, with DRPA applied, the percentage increase in average SE for the strong user at high SNRs is $(M_N - \hat{R}_1)/\hat{R}_1$.

Fig. 8 depicts the average SE versus transmit SNR for *Scheme 2* with and without DRPA algorithm. It is shown that the strong user's average SE in *Scheme 2* is unaffected by the DRPA algorithm. However, with DRPA applied, the weak user's average SE in *Scheme 2* is larger than that without DRPA, especially at high SNRs. For example, when the transmit SNR is 70 dB, the average SE achieved with DRPA for the weak user in *Scheme 2* is 8 times larger than that obtained without DRPA. This is because, when there is no DRPA, the weak user's average SE in *Scheme 2* is bounded by the minimum target rate, i.e., $\hat{R}_2$ or $\log_2(\theta_2)$, which equals 1 b/s/Hz according to our parameter settings. Nevertheless, Fig. 8 shows that when the DRPA algorithm is utilized, the weak user's average SE in *Scheme 2* continues to increase until it reaches the highest rate due to practical system limitations on modulation order. With DRPA applied, the percentage increase in average SE for the weak user in *Scheme 2* at high SNRs is $(M_N - \hat{R}_2)/\hat{R}_2$.

Fig. 9 depicts the total average SE versus transmit SNR for *Scheme 1* and *Scheme 2*, with and without DRPA algorithm, compared with the fixed power allocation scheme. The minimum target rates, i.e., $\hat{R}_1$ and $\hat{R}_2$, are set to 2 b/s/Hz and 1 b/s/Hz. Fig. 9 shows that the fixed power allocation scheme achieves the smallest total average SE among all the schemes, while with the proposed DRPA algorithm applied to the two power

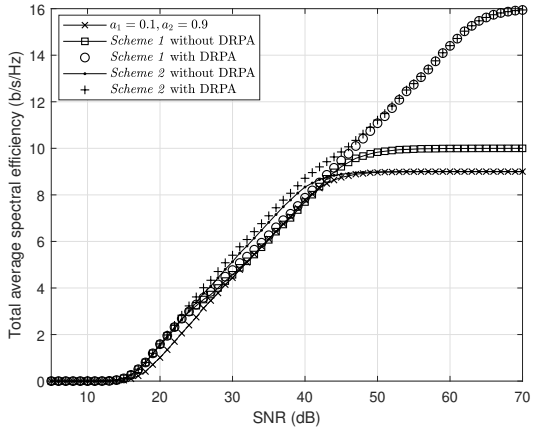


Fig. 9: Total average SE versus transmit SNR, for *Scheme 1*, *Scheme 2* with and without DRPA and fixed power coefficients ($a_1 = 0.1$, $a_2 = 0.9$), where $\hat{R}_1 = 2$ b/s/Hz and $\hat{R}_2 = 1$ b/s/Hz.

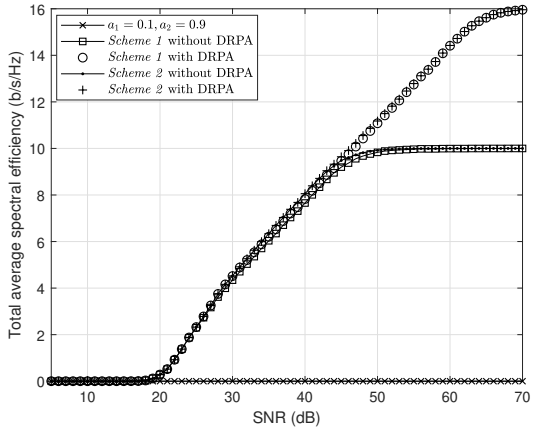


Fig. 10: Total average SE versus transmit SNR, for *Scheme 1*, *Scheme 2* with and without DRPA and fixed power coefficients ($a_1 = 0.1$, $a_2 = 0.9$), where $\hat{R}_1 = 2$ b/s/Hz and $\hat{R}_2 = 2$ b/s/Hz.

adaptation schemes, they achieve the largest total average SE at high SNRs. Although Fig. 9 shows that at high SNRs, the fixed power allocation scheme and the *Scheme 2* without DRPA converge to the same average SE value, this is not always the case.

Finally, Fig. 10 is plotted to show the performance of total average SE for *Scheme 1* and *Scheme 2*, with and without DRPA algorithm. The total average SE for the fixed power coefficients with $a_1 = 0.1$, $a_2 = 0.9$ is also illustrated. The minimum target rates, i.e., $\hat{R}_1$ and $\hat{R}_2$, are set to 2 b/s/Hz and 2 b/s/Hz. Firstly, it can be noticed that the total average SE for the considered fixed power coefficients scheme is zero. Since the average SE considered in this paper is the rate satisfying the minimum rate constraint, this indicates that the considered fixed power coefficients, i.e., $a_1 = 0.1$, $a_2 = 0.9$, cannot guarantee the minimum required rates. This actually reflects the benefits of adaptive power strategies which can take advantage of favourable channel conditions and adapt to flexible rate guarantees. Fig. 10 also shows that with DRPA applied, both power adaptation schemes achieve much better performance in terms of total average SE, especially at high SNRs. When the transmit SNR is 70 dB, the total average SE achieved with DRPA is 1.6 times larger than that obtained without DRPA. It validates the effectiveness of our algorithm.

## V. Conclusions

Joint adaptive transmission considering practical adaptive M-QAM modulation and power adaptation strategies was investigated in this paper for a downlink two-user NOMA network. It is noted that for a given BER requirement, the constellation size, as a function of channel fading and power allocation, can be adjusted. Hence, we proposed two adaptive power allocation schemes that take advantage of favourable channel conditions and guarantee the minimum rate constraints. The performance of joint adaptive transmission was then studied, by considering adaptive continuous-rate modulation and discrete-rate modulation. It was found that for discrete-rate modulation, the average SEs for both users in both power schemes are bounded, while for the weak user in *Scheme 1* and the strong user in *Scheme 2*, their average SEs are unbounded. This is because for practical discrete-rate modulations, commonly used in cellular networks, the available constellation sizes are discrete and there exists a highest modulation order due to system limitations. With the aim to further increase the total transmission rate, a DRPA algorithm was proposed. Simulation results validated the effectiveness of the proposed algorithm, allowing both users in each scheme to reach the highest modulation order at high SNRs.

## Appendix A

### Proof for Theorem 1

From III-A1, it can be noted that in *Scheme 1*, the instantaneous transmitting rate of strong user is always kept at the minimum required rate, indicating that $\bar{R}_1 =$

$\mathrm{E}[\log_2(\theta_1)]$. Based on (24), (25), and (26a), we have that

$$\begin{aligned}\bar{R}_1 &= \int_{l_1}^{l_2}\int_{l_3}^{\infty} \log_2(\theta_1) 2e^{-g_1}e^{-g_2}\mathrm{d}g_1\mathrm{d}g_2 \\ &\quad + \int_{l_2}^{\infty}\int_{l_4}^{\infty} \log_2(\theta_1) 2e^{-g_1}e^{-g_2}\mathrm{d}g_1\mathrm{d}g_2, \qquad (55a)\\ &= \int_{l_1}^{l_2} 2e^{-g_2-l_3}\log_2(\theta_1)\mathrm{d}g_2 + \log_2(\theta_1)e^{-2l_2}. \qquad (55b)\end{aligned}$$

Then, based on (24), (25), and (26b), the average SE for the weak user in *Scheme 1* can be expressed as

$$\begin{aligned}\bar{R}_2 &= \int_{l_1}^{l_2}\int_{l_3}^{\infty} \log_2\left(1+K\frac{\gamma_\mathrm{t} a_{2\mathrm{upper}}(g_1)g_2}{1+\gamma_\mathrm{t} a_{1\mathrm{low}}(g_1)g_2}\right) \\ &\quad \times 2e^{-g_1}e^{-g_2}\mathrm{d}g_1\mathrm{d}g_2 \\ &\quad + \int_{l_2}^{\infty}\int_{l_4}^{\infty} \log_2\left(1+K\frac{\gamma_\mathrm{t} a_{2\mathrm{upper}}(g_1)g_2}{1+\gamma_\mathrm{t} a_{1\mathrm{low}}(g_1)g_2}\right) \\ &\quad \times 2e^{-g_1}e^{-g_2}\mathrm{d}g_1\mathrm{d}g_2, \qquad (56)\end{aligned}$$

where $l_1 = \frac{\theta_2-1}{K\gamma_\mathrm{t}}$, $l_2 = \frac{(\theta_2-1+K)(\theta_1-1)+K(\theta_2-1)}{K^2\gamma_\mathrm{t}}$, $l_3 = \frac{g_2(\theta_2-1+K)(\theta_1-1)}{K(K\gamma_\mathrm{t}g_2-\theta_2+1)}$, $l_4 = g_2$.

Now let us consider *Scheme 2*. From III-A2, it can be noted that in *Scheme 2*, the instantaneous transmitting rate of weak user always stays at the minimum required rate, which means that $\bar{R}_2 = \mathrm{E}[\log_2(\theta_2)]$. Similar to the above analysis, it can be then written as

$$\bar{R}_2 = \int_{l_1}^{l_2} 2e^{-g_2-l_3}\log_2(\theta_2)\mathrm{d}g_2 + \log_2(\theta_2)e^{-2l_2}. \quad (57)$$

Based on (24), (25), and (26a), the average SE for the strong user in *Scheme 2* can be expressed as

$$\begin{aligned}\bar{R}_1 &= \int_{l_1}^{l_2}\int_{l_3}^{\infty} \log_2\left(1+K\gamma_\mathrm{t} a_{1\mathrm{upper}}(g_2)g_1\right) \\ &\quad \times 2e^{-g_1}e^{-g_2}\mathrm{d}g_1\mathrm{d}g_2 \\ &\quad + \int_{l_2}^{\infty}\int_{l_4}^{\infty} \log_2\left(1+K\gamma_\mathrm{t} a_{1\mathrm{upper}}(g_2)g_1\right) \\ &\quad \times 2e^{-g_1}e^{-g_2}\mathrm{d}g_1\mathrm{d}g_2. \qquad (58)\end{aligned}$$

By inserting $a_{1\mathrm{upper}}(g_2)$ and by defining $t = \frac{K(K\gamma_\mathrm{t}g_2-\theta_2+1)}{(\theta_2-1+K)g_2}$, (58) can be written as

$$\begin{aligned}\bar{R}_1 &= \int_{l_1}^{l_2} 2e^{-g_2}\int_{l_3}^{\infty} \log_2(1+tg_1)e^{-g_1}\mathrm{d}g_1\mathrm{d}g_2 \\ &\quad + \int_{l_2}^{\infty} 2e^{-g_2}\int_{l_4}^{\infty} \log_2(1+tg_1)e^{-g_1}\mathrm{d}g_1\mathrm{d}g_2. \qquad (59)\end{aligned}$$

## APPENDIX B
## PROOF FOR LEMMA 2

From the definitions of $l_1$, $l_2$, $l_3$, $l_4$ in Theorem 1, we can find that when the transmit SNR $\gamma_\mathrm{t} \to \infty$, $l_1 \to 0$, $l_2 \to 0$, $l_3 \to 0$, $l_4 = g_2$. Therefore, for the strong user in *Scheme 1*, we get that

$$\begin{aligned}\bar{R}_1 &\xrightarrow{\gamma_\mathrm{t}\to\infty} \int_0^{\infty}\int_{g_2}^{\infty} \log_2(\theta_1) 2e^{-g_1}e^{-g_2}\mathrm{d}g_1\mathrm{d}g_2 \\ &= 2\log_2(\theta_1)\int_0^{\infty} e^{-2g_2}\mathrm{d}g_2 = \log_2(\theta_1). \qquad (60)\end{aligned}$$

By inserting $a_{2\mathrm{upper}}(g_1)$, when $\gamma_\mathrm{t} \to \infty$, the average SE for the weak user in *Scheme 1* becomes

$$\begin{aligned}\bar{R}_2 &\xrightarrow{\gamma_\mathrm{t}\to\infty} \int_0^{\infty}\int_{g_2}^{\infty} \log_2\left(1+K\frac{g_2\left(K\gamma_\mathrm{t}g_1-\theta_1+1\right)}{Kg_1+g_2(\theta_1-1)}\right) \\ &\quad \times 2e^{-g_1}e^{-g_2}\mathrm{d}g_1\mathrm{d}g_2 \xrightarrow{\gamma_\mathrm{t}\to\infty} \infty. \qquad (61)\end{aligned}$$

Hence, we prove that for *Scheme 1*, when $\gamma_\mathrm{t} \to \infty$, $\lim_{\gamma_\mathrm{t}\to\infty} \bar{R}_1 = \log_2(\theta_1)$, $\lim_{\gamma_\mathrm{t}\to\infty} \bar{R}_2 \to \infty$. For *Scheme 2*, the analysis can be done in a similar way, which is omitted here.

## REFERENCES


[1] Y. Liu, Z. Qin, M. Elkashlan, Z. Ding, A. Nallanathan, and L. Hanzo, "Non-orthogonal multiple access for 5G and beyond," *Proceedings of the IEEE*, vol. 105, no. 12, pp. 2347–2381, Dec. 2017.

[2] W. Yu, L. Musavian, and Q. Ni, "Link-layer capacity of NOMA under statistical delay QoS guarantees," *IEEE Trans. Commun.*, vol. 66, no. 10, pp. 4907–4922, Oct. 2018.

[3] W. Hao, M. Zeng, Z. Chu, and S. Yang, "Energy-efficient power allocation in millimeter wave massive MIMO with non-orthogonal multiple access," *IEEE Wireless Communications Letters*, vol. 6, no. 6, pp. 782–785, 2017.

[4] L. Dai, B. Wang, M. Peng, and S. Chen, "Hybrid precoding-based millimeter-wave massive MIMO-NOMA with simultaneous wireless information and power transfer," *IEEE Journal on Selected Areas in Communications*, vol. 37, no. 1, pp. 131–141, 2019.

[5] J. Cui, Z. Ding, and P. Fan, "Outage probability constrained MIMO-NOMA designs under imperfect CSI," *IEEE Transactions on Wireless Communications*, vol. 17, no. 12, pp. 8239–8255, 2018.

[6] T. Q. Duong, X. Zhou, and H. V. Poor, *Trusted Communications with Physical Layer Security for 5G and Beyond*. Inst. of Eng. and Technol., Nov. 2017.

[7] W. Yu, A. Chorti, L. Musavian, H. V. Poor, and Q. Ni, "Effective secrecy rate for a downlink NOMA network," *IEEE Trans. Wireless Commun.*, vol. 18, no. 12, pp. 5673–5690, Dec. 2019.

[8] L. Lv, H. Jiang, Z. Ding, L. Yang, and J. Chen, "Secrecy-enhancing design for cooperative downlink and uplink NOMA with an untrusted relay," *IEEE Transactions on Communications*, vol. 68, no. 3, pp. 1698–1715, 2020.

[9] M. Amjad, L. Musavian, and S. Aïssa, "NOMA versus OMA in finite blocklength regime: Link-layer rate performance," *IEEE Transactions on Vehicular Technology*, vol. 69, no. 12, pp. 16 253–16 257, 2020.

[10] L. Yang, H. Jiang, Q. Ye, Z. Ding, L. Lv, and J. Chen, "On the impact of user scheduling on diversity and fairness in cooperative NOMA," *IEEE Transactions on Vehicular Technology*, vol. 67, no. 11, pp. 11 296–11 301, 2018.

[11] B. Su, Q. Ni, W. Yu, and H. Pervaiz, "Optimizing computation efficiency for NOMA-assisted mobile edge computing with user cooperation," *IEEE Transactions on Green Communications and Networking*, pp. 1–1, 2021.

[12] P. Popovski, K. F. Trillingsgaard, O. Simeone, and G. Durisi, "5G wireless network slicing for eMBB, URLLC, and mMTC: A communication-theoretic view," *IEEE Access*, vol. 6, pp. 55 765–55 779, 2018.

[13] M. Shirvanimoghaddam, M. Condoluci, M. Dohler, and S. J. Johnson, "On the fundamental limits of random non-orthogonal multiple access in cellular massive IoT," *IEEE J. Sel. Areas Commun.*, vol. 35, no. 10, pp. 2238–2252, Oct. 2017.

[14] J. Choi, "NOMA-based random access with multi-channel ALOHA," *IEEE J. Sel. Areas Commun.*, vol. 35, no. 12, pp. 2736–2743, Dec. 2017.

[15] E. Balevi, F. T. A. Rabee, and R. D. Gitlin, "ALOHA-NOMA for massive machine-to-machine IoT communication," in *Proc. IEEE Int. Conf. Commun. (ICC)*, Kansas City, MO, USA, May 2018.

[16] L. Miuccio, D. Panno, and S. Riolo, "Joint control of random access and dynamic uplink resource dimensioning for massive MTC in 5G NR based on SCMA," *IEEE Internet Things J.*, vol. 7, no. 6, pp. 5042–5063, Jun. 2020.

[17] W. Yu, C. H. Foh, A. ul Quddus, Y. Liu, and R. Tafazolli, "Throughput analysis and user barring design for uplink NOMA-enabled random access," 2020.

[18] A. J. Goldsmith and Soon-Ghee Chua, "Variable-rate variable-power MQAM for fading channels," *IEEE Transactions on Communications*, vol. 45, no. 10, pp. 1218–1230, Oct 1997.

[19] H. Jia and L. Musavian, "Performance analysis for NOMA with M-QAM modulation," in *2020 IEEE 91st Vehicular Technology Conference (VTC2020-Spring)*, 2020, pp. 1–5.

[20] A. J. Goldsmith, *Wireless Communications*. Cambridge: Cambridge Univ. Press, 2005.

[21] T. L. Marzetta and B. M. Hochwald, "Fast transfer of channel state information in wireless systems," *IEEE Transactions on Signal Processing*, vol. 54, no. 4, pp. 1268–1278, 2006.

[22] Z. Ding, Z. Yang, P. Fan, and H. V. Poor, "On the performance of non-orthogonal multiple access in 5g systems with randomly deployed users," *IEEE Signal Processing Letters*, vol. 21, no. 12, pp. 1501–1505, Dec 2014.

[23] H. A. David and H. N. Nagaraja, *Order Statistics*. John Wiley, New York, 3rd ed., 2003.